A New Approach To Gas Discharge Theory With Sheath Boundaries

Francis F. Chen* and Davide Curreli[1]

University of California, Los Angeles.
[1]*University of Illinois at Urbana Champaign*

E-mail: ffchen@ee.ucla.edu, dcurreli@illinois.edu

Classical theories of gas discharges have concentrated on the microscopic properties of collisions and diffusion coefficients, but few have considered the macroscopic observables such as the density and temperature profiles. Since practical devices cannot be approximated by infinite cylinders, we consider finite cylinders with endplates. There, the short-circuit effect permits electrons to be Maxwellian even in the presence of a DC magnetic field. For uniform electron temperature T_e and pressure p, the radial density profile is found to have a "universal" shape independent of p. A code EQM is developed to solve for radial profiles when all quantities vary with r and includes ionization balance and neutral depletion. The profile $T_e(r)$ depends on the type of discharge and is found for helicon discharges by iterating with the code HELIC. Resulting $n(r)$ profiles are flat or peaked on axis, as found in experiment, even when ionization is localized to the edge.

1. Introduction and ion motion

Partially ionized plasmas, known as gas discharges, have been studied for many decades but have taken on widespread interest now that they are used in the production of semiconductor circuits. The literature on gas discharge theory is extensive. Most theorists [1,2], treat microscopic quantities such as cross sections and diffusion coefficients, since positive columns were the main source of early experimental data. A few recent papers [3] consider also the macroscopic quantities such as the steady-state density profile. The difficulty is that the particular geometry of the plasma container (henceforth called "tube") affects the results. Here we sidestep the issue by adopting a simple model which retains only the essential features of a discharge while omitting effects which do not change the general nature of the solution. A cylinder reduces the problem to one dimension, but there are no infinite cylinders. We therefore assume the finite-length cylinder shown in Fig. 1. The boundary conditions at the ends entail sheath theory.
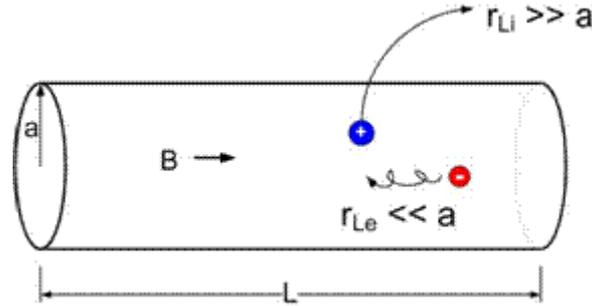
Fig. 1.   The assumed tube geometry.

The cylinder has radius a and length L, and there is a uniform DC magnetic field (B-field), in the z direction.   The B-field has intermediate strength such that the ion Larmor radius at electron temperature T_e is much larger than a, and the electron Larmor radius much smaller than a.   We can then neglect the curvature of the ion orbits and the diffusion of electrons across **B**.   We also assume $T_i << T_e$ so that T_i can be neglected. The ion fluid equation is given by [4]

$$M\mathbf{v}\nabla \cdot (n\mathbf{v}) + Mn\mathbf{v}\cdot\nabla\mathbf{v} - en\mathbf{E} + Mnv_{io}\mathbf{v} = en(\mathbf{v}\times\mathbf{B}) - KT_i\nabla n \approx 0 . \tag{1}$$

The terms on the right-hand side will be neglected, as explained above.   The first term on the left side represents ion drag due to ionization, since ions are born near zero velocity.   Though this term will be replaced by the equation of continuity, it is shown here because it conveniently avoids the task of keeping track of how ions born at each radius are accelerated by the radial electric field (E-field).   The ionization and charge-exchange collision probabilities are

$$P_i(r) \equiv <\sigma v>_{ion}(r), \quad P_c(r) \equiv <\sigma v>_{cx}(r) = v_{io}/n_n . \tag{2}$$

The equation of continuity can be written

$$\nabla \cdot (n\mathbf{v}) = nn_n P_i(r), \tag{3}$$

where n_n is the density of neutrals.   Eq. (1) now becomes

$$M\mathbf{v}\cdot\nabla\mathbf{v} - e\mathbf{E} + Mn_n(P_i + P_c)\mathbf{v} = 0, \tag{4}$$

or, in one dimension, the ion equation of motion is

$$v\frac{dv}{dr} = c_s^2\frac{d\eta}{dr} - n_n(P_c + P_i)v, \tag{5}$$

where we have dropped the subscript on v_r and have used the usual definitions

$$\mathbf{E} \equiv -\nabla\phi, \quad \eta \equiv -e\phi/KT_e, \quad \text{and} \quad c_s \equiv (KT_e/M)^{\frac{1}{2}} . \tag{6}$$

The radial component of Eq. (3) is our ion equation of continuity:

$$\frac{dv}{dr} + v\frac{d(\ln n)}{dr} + \frac{v}{r} = n_n P_i(r) . \tag{7}$$

II.   Electron motion

In our experiments on helicon waves, we always find that the electron distribution is Mawellian [Eq. (8)], even in a strong B-field.   If the density is peaked on axis, as it most often is, and if the plasma is ionized near the edge, how do the electrons get across B to the center?   They do this by the Simon short-circuit effect [5]. Since real plasmas have finite length, they have endplates, and there are sheaths on the endplates.   This is shown in Fig. 2, where ionization occurs near the edge.   Electrons cross **B** very slowly, but those that follow the ions can be confined longer by thicker sheaths at the ends.   The electrons seem to cross the field with the ions, but they are actually confined by varying sheath drops as they bounce back and forth between endplates in nanoseconds.

$$n = n_0 e^{e\phi/KT_e} = n_0 e^{-\eta} .$$
(8)

In Eq. (8) the temperature T_e can vary with r as electrons are created at different radii, by different RF field strengths, for instance.
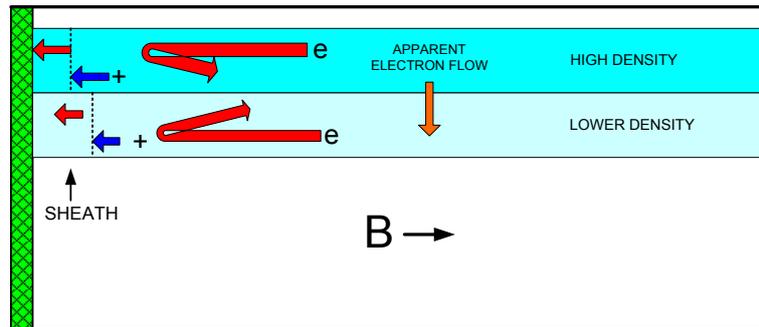

Fig. 2.   The short-circuit effect.

III.   A "universal" profile

The derivative of Eq. (8) can be written

$$\frac{d(\ln n)}{dr} = -\frac{d\eta}{dr} .$$
(10)

Inserting this into Eq. (7) gives

$$\frac{dv}{dr} - v\frac{d\eta}{dr} + \frac{v}{r} = n_n P_i(r).$$
(11)

With $d\eta/dr$ solved from Eq. (5), this can be written

$$\frac{dv}{dr} + \frac{v}{r} - \frac{v^2}{c_s^2}\left[\frac{dv}{dr} + n_n(P_i + P_c)\right] = n_n P_i(r) . \tag{12}$$

Solving for dv/dr, we obtain the following ordinary, first-order differential equation for the ion fluid velocity v:

$$\frac{dv}{dr} = \frac{c_s^2}{c_s^2 - v^2}\left[-\frac{v}{r} + n_n P_i + \frac{v^2}{c_s^2} n_n(P_i + P_c)\right]. \tag{13}$$

Note that dv/dr diverges as v approaches c_s, giving us a natural transition to the Debye sheath at $r \approx a$. Numerical solutions of Eq. (13) can account for all quantities varying with r.

To see the nature of this equation, we first normalize v to c_s,

$$u \equiv v / c_s , \tag{14}$$

obtaining

$$\frac{du}{dr} = \frac{1}{1-u^2}\left\{-\frac{u}{r} + \frac{n_n}{c_s} P_i\left[1 + u^2(1 + P_c / P_i)\right]\right\}. \tag{15}$$

We next define

$$k(r) \equiv 1 + P_c(r) / P_i(r) \tag{16}$$

to obtain

$$\frac{du}{dr} = \frac{1}{1-u^2}\left[-\frac{u}{r} + \frac{n_n}{c_s} P_i(1 + ku^2)\right]. \tag{17}$$

The coefficient in the last term can be removed by normalizing the radius r to ρ:

$$\rho \equiv (n_n P_i / c_s)r , \tag{18}$$

whence

$$\frac{du}{d\rho} = \frac{1}{1-u^2}\left[1 + ku^2 - \frac{u}{\rho}\right]. \tag{19}$$

Note that all the properties of the plasma are contained in $k(r)$, and the only relevant property is the ratio P_c/P_i, which occurs only in the nonlinear term arising originally

from the $\mathbf{v} \cdot \nabla \mathbf{v}$ term in Eq.(1).

IV.   Solutions for uniform T_e and pressure p (constant k)

Pressure is given here in mTorr, where 1 mTorr corresponds to $n_n = 3.3 \times 10^{13}$ cm^{-3}.   Figure 3 shows solutions of Eq. (19) for three different values of k.   Each curve of u goes to infinity at a different radius ρ_a, which is to be identified with the sheath edge at $r = a$.   If we rescale ρ in each case so that ρ_a corresponds to $r = a$, all the curves become identical regardless of k, as shown in Fig. 4.   These profiles are universal in the sense that they do not depend on the size a of the plasma or the pressure p, since k is independent of n_n.
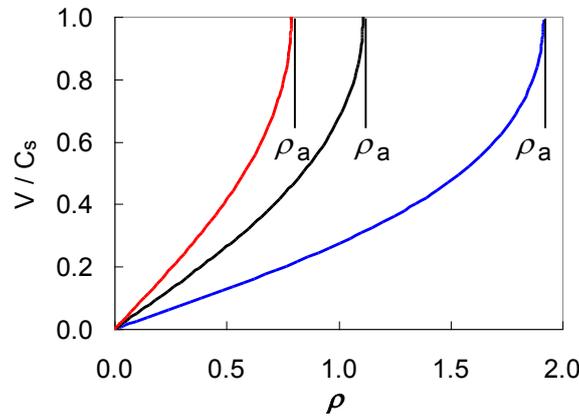

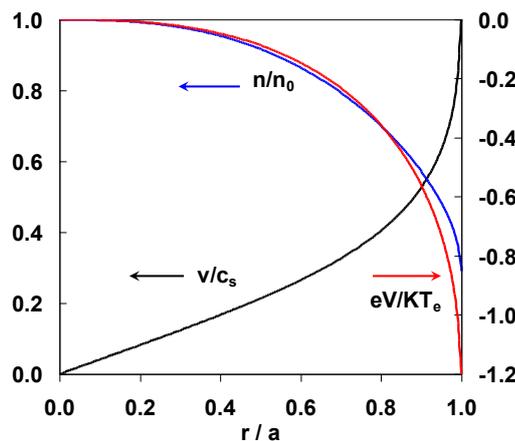Fig. 3.   Solutions of Eq. (19) for three values of k.

Fig. 4.   The "universal" profiles.

Temperature and pressure cannot be varied independently because of ionization balance.   Consider a cylindrical shell of width dr at r.   The total input of ions into the shell per unit length (with $n_e = n_i = n$) is

$$\frac{dn_T(r)}{dt} = 2\pi r dr \cdot n(r) n_n(r) \cdot <\sigma v>_{ion} (T_e) \tag{20}$$

The total outflow from the shell is

$$-\frac{dn_T(r)}{dt} = 2\pi r dr \nabla \cdot [n(r)v(r)] = 2\pi r dr \cdot \frac{1}{r}\frac{d}{dr}[rn(r)v(r)]. \tag{21}$$

Equating these gives

$$\frac{1}{nr}\frac{d}{dr}(rnv) = n_n P_i(T_e). \tag{22}$$

When this is solved with Eq. (17) for a dimensional discharge radius r, only one value of KT_e will have $u \to \infty$ at $r \approx a$. This is shown in Fig. 5. Repeating this for various pressures yields the familiar curves of Fig. 6 showing the inverse dependence of KT_e on p for various a. These curves account for local dependences, whereas previously only radial averages could be used.
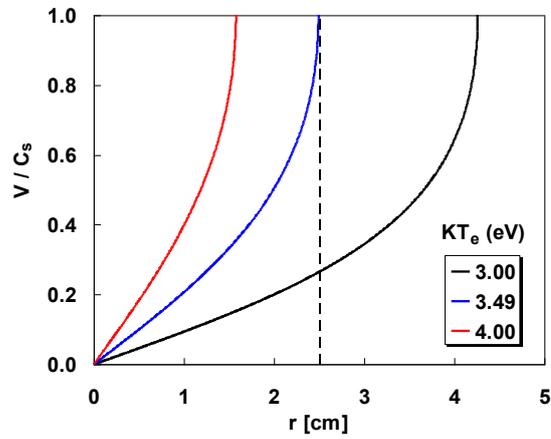
Fig. 5.   Profiles of $u(r)$ in a 2.5-cm radius, 10-mTorr argon discharge. Only one value of T_e gives the right position for the sheath edge.
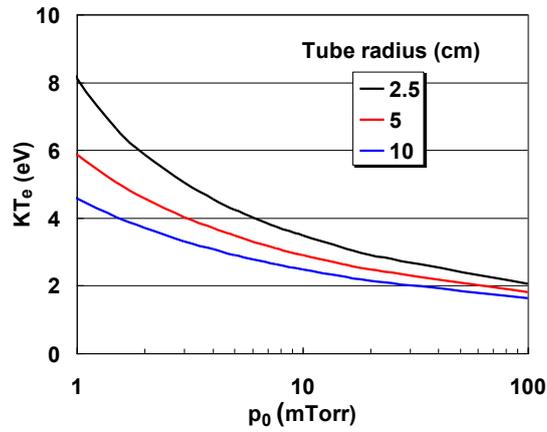

Fig. 6.   Relation between T_e and pressure in argon discharges of various radii.

Since T_e varies with p, radial profiles are no longer independent of pressure.   Figure 7 shows the density profiles at three pressures when the corresponding T_e's are used.
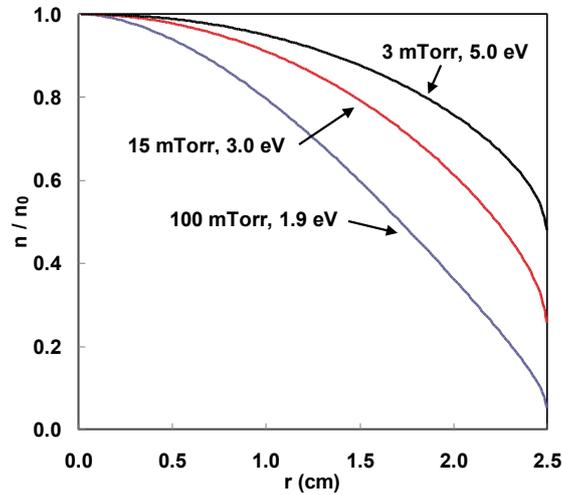
Fig. 7.   Density profiles at three pressures, computed with the corresponding KT_e given in Fig. 5 for $a =$ 2.5 cm.

V.   Further developments

So far, we have the mechanism for calculating equilibrium profiles for given functions $T_e(r)$ and $n_n(r)$, but these are not yet specified.   To obtain $n_n(r)$, neutral depletion was computed in our full paper [6] by using a simple model.   An example of the results is shown in Fig. 8
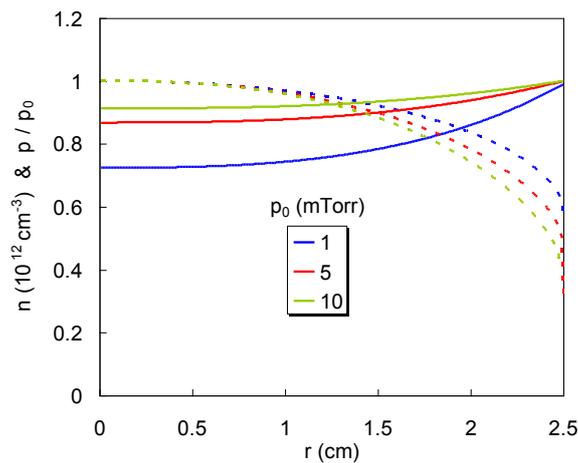

Fig. 8.   Neutral pressure profiles (solid lines) for argon discharges in a 5-cm diam tube with initial pressures $p_0 = 1$, 5, and 10 mTorr at 400K.   The corresponding plasma density profiles peaked at 10^{12} cm^{-3} are shown by the dashed curves.
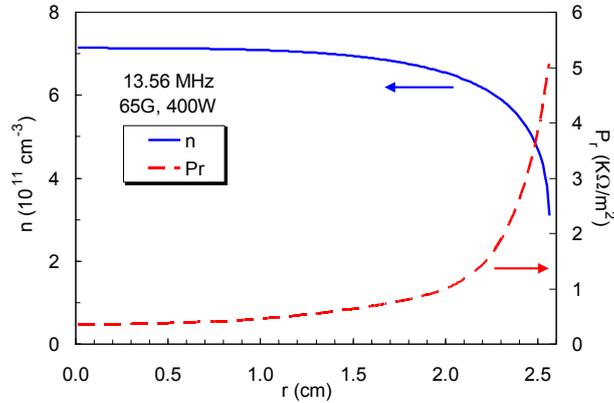
Fig. 9.   Curves of $n(r)$ (——) and $P_r(r)$ (- - -), obtained by iteration of EQM with HELIC, for a 15-mTorr helicon discharge at 65G with 400W of RF at 13.56 MHz and an $m = 0$ antenna.

To obtain $T_e(r)$ requires knowing the ionization mechanism and, therefore the type of discharge.   We have used the helicon discharge, since a code HELIC has been devised by Arnush [7] to describe these discharges in detail.   We have written a code EQM to solve the equations given in this paper.   This code provides equilibrium $n(r)$ and $n_n(r)$ profiles as inputs to HELIC, and the latter then computes $T_e(r)$.   By iterating between EQM and HELIC, we can show that $n(r)$ always peaks on axis, in agreement with experiment, even though power deposition $P_r(r)$ is at the edge due to the Trivelpiece-Gould mode.   Physically, $n(r)$ *must* peak at the center, since the Boltzmann relation then requires the potential to peak there, leading to an outward pointing E-field to drive the ion out radially.   Ion loss by axial diffusion at temperature T_i would be too slow.

VI.   Summary

The old problem of "anomalous skin depth", in which plasma densities peaking at the center can be created by RF energy applied only at the edge, has been solved. The endplates of finite-length plasmas are treated with sheath theory.   Automatic adjustments of the sheath drops during the approach to equilibrium create an inward E-field that drives ions into the center.   After equilibrium is reached, the plasma density is peaked at the center, or at least flat and not hollow, so that an outward E-field pushes the ions outward when radial losses dominate over axial ones.

VII.   Acknowledgments

References

[1]　L.D. Tsendin, Plasma Sources Sci. Technol. **20**, 055011 (2011).
[2]　R.E. Robson, R.D. White, and Z.Lj. Petrović, Rev. Mod. Phys. 77, 1303 (2005).
[3]　A. Fruchtman, G. Makrinich, and J. Ashkenazy,　Plasma Sources Sci. Technol. **14**, 152 (2005).
[3]　F.F. Chen, *Intro. to Plasma Physics and Controlled Fusion,* Vol. 1, 2nd ed. (Plenum, New York, 1984), p. 239.
[4]　A. Simon, Phys. Rev. **98**, 317 (1955).
[5]　D. Curreli and F.F. Chen, Phys. Plasmas **18**, 113501 (2011).
[6]　D. Arnush, Phys. Plasmas **7**, 3042 (2000).